

Real time cantilever signal frequency determination using digital signal processing

Yu. Obukhov, K. C. Fong, D. Daughton, and P. C. Hammel

Department of Physics, The Ohio State University, Columbus, Ohio 43210

(Received 11 July 2006; accepted 6 December 2006; published online 13 February 2007)

We describe a digital signal processing method for high precision frequency evaluation of approximately sinusoidal signals based on a computationally efficient method. We demonstrate frequency measurement enabling sensitive measurement of the oscillatory force exerted on a micromechanical cantilever. We apply this technique to detection of the force signal arising in a micromechanically detected magnetic resonance force microscopy electron spin resonance signal. Our frequency detection measurements agree well with the theoretical noise analysis presented here, and we find that due to the excellent sensitivity of optical displacement detection, our sensitivity is limited only by the thermal displacement noise of the cantilever. © 2007 American Institute of Physics. [DOI: 10.1063/1.2434955]

I. INTRODUCTION

Magnetic resonance force microscopy (MRFM), an emerging scanned probe magnetic resonance technique that combines the strengths of magnetic resonance imaging (MRI) and scanned force microscopy (SFM),¹ is a topic of intense research. The recent demonstration of force detection of the magnetic resonance signal of a single electron spin² is a milestone that has increased interest in this topic.

An essential strength of MRFM is its excellent sensitivity to the small forces exerted by spins that are manipulated using microwave fields. The force sensor is a micromechanical resonator (microcantilever) with high quality factor Q . A force applied to the microcantilever at its eigenfrequency ω_0 produces an oscillatory response whose amplitude is Q times larger than for a nonresonant force. One can use the cantilever amplitude to sensitively measure the force, but this is only useful for variations of the force slower than the resonator response time ($\sim 2Q/\omega_0$) (while the effective Q can be reduced by negative feedback techniques,³ the modified limit on the response time remains). This limitation can be circumvented by detecting the shift in either the frequency or the phase of the oscillating cantilever in response to a force⁴ rather than its amplitude: An oscillatory force applied to the oscillating cantilever in phase with its displacement will shift the eigenfrequency of the cantilever in proportion to the applied force. The eigenfrequency responds immediately to the applied force thus circumventing the bandwidth limitations associated with amplitude detection.

Earlier implementations of frequency detection⁴ employed an electronic tank circuit in combination with a positive feedback self-oscillation circuit based on a phase shifter and automatic gain control amplifier. This method has advantages and disadvantages which we discuss in more detail below, however, thermal drift of tank circuit component values can hinder high resolution frequency measurement; a digital approach eliminates this problem.

Here we propose a previously unrecognized approach to digital frequency evaluation of a cantilever signal that can be implemented in a real-time measurement system, and that

demonstrates sensitivity predominantly determined by intrinsic thermally excited noise in the cantilever signal frequency. This method is useful not only for MRFM but for any SFM system. First we describe the principles of our frequency evaluation method for the case of a sinusoidal signal. In the second section we analyze the consequences of noise (we consider the regime in which the noise is small compared to the signal and so the signal remains approximately sinusoidal) and discuss the limits of the method as applied to cantilever based force measurements. In the third section we describe an implementation of the frequency detection system using digital signal processing hardware. In the final section we demonstrate the performance of the system through application to the detection of an electron spin resonance (ESR) signal using MRFM.

II. FREQUENCY EVALUATION FOR SINUSOIDAL SIGNALS

We first present our method for evaluating the frequency of a sinusoidal signal $x(t)$; below we analyze the consequences of small departures from ideal sinusoidal behavior resulting from, e.g., noise,

$$x = x_0 \sin(\omega_0 t + \phi),$$

where ω_0 and ϕ are the frequency and phase of the signal and x_0 is the signal amplitude. The linear relationship between x and its second derivative

$$\ddot{x} = -\omega_0^2 x$$

allows us to extract the frequency ω_0 from a linear fit of \ddot{x} to x .

If we periodically sample the signal x with a time interval Δt we generate a set of N points

$$\{x_i\} = \{x_0 \sin(\omega_0 \Delta t i + \phi)\},$$

where the integer $i \leq N$. To pursue this strategy for obtaining ω_0 from a digital record we define the digital derivative of x_i as

$$\dot{x}_i = \frac{x_{i+1} - x_{i-1}}{2\Delta t}$$

and the results for a nearly sinusoidal signal x are

$$\begin{aligned}\dot{x}_i &= \frac{x_0}{2\Delta t} [\sin(\omega_0 \Delta t(i+1) + \phi) - \sin(\omega_0 \Delta t(i-1) + \phi)] \\ &= x_0 \frac{\sin(\omega_0 \Delta t)}{\Delta t} \cos(\omega_0 \Delta t i + \phi)\end{aligned}$$

and

$$\ddot{x}_i = -x_0 \frac{\sin^2(\omega_0 \Delta t)}{\Delta t^2} \sin(\omega_0 \Delta t i + \phi) = -\frac{\sin^2(\omega_0 \Delta t)}{\Delta t^2} x_i.$$

We can then obtain ω_0 from a linear fit of $\{\ddot{x}_i\}$ to $\{x_i\}$ (each record containing N points). Least mean squares fitting gives the fit value A

$$A = \frac{\sin^2(\omega_0 \Delta t)}{\Delta t^2} = -\frac{\sum_{i=1}^N \ddot{x}_i \cdot x_i}{\sum_{i=1}^N x_i^2}, \quad (1)$$

hence

$$f_0 = \frac{1}{2\pi\Delta t} \arcsin(\Delta t \sqrt{A}).$$

This approach allows determination of the frequency of a nearly sinusoidal digital record. This method has clear advantages in comparison, for example, with a standard counter which is based upon measuring the time interval between crossings of the signal at some trigger value. In the present case, the signal frequency is determined from a collection of sampled points made with only a few points per signal period. Every point collected contributes to determining the frequency, not only those near the trigger level. The sampling rate can be small in comparison to the high frequency (relative to the signal frequency) usually used for precise measurement of time interval between two signal crossings.

We can also compare to the traditional method of analog frequency demodulation discussed in Ref. 5 in which the oscillatory signal is applied to a RLC tank circuit whose resonance frequency is near the frequency to be measured; the result is an output voltage whose phase, relative to the input, is very sensitive to signal frequency. By measuring this phase difference the frequency of input signal can be determined. This scheme can be implemented digitally by means of an algorithm that simulates the tank circuit, and this provides equivalently accurate frequency determination limited only by the signal-to-noise-ratio (SNR) of the input signal. However, the scheme we present has the advantage of being more direct and hence requiring smaller computation time compared to the digital tank circuit implementation. The analog approach is relatively easy to implement and works well with high frequency signals, but to achieve high frequency resolution the width of the analog tank circuit resonance must be small, and this can lead to problems associated with thermal drift of analog components, a factor that is eliminated in a digital implementation. On the other

hand, the maximum frequency signal manageable by the digital scheme is limited for real time operation by the computation speed of the digital signal processing unit.

In principle, a sampling rate prescribed by the Nyquist theorem (not less than two points per period: $\omega_0 \Delta t < \pi$) is required to operate reliably. However, as $\omega_0 \Delta t \rightarrow \pi$ the value $-\sin^2(\omega_0 \Delta t)/\Delta t^2 \rightarrow 0$, yet the impact of noise on the fitting remains the same so the SNR can be substantially reduced. We propose the more practical rate $\omega_0 \Delta t \leq \pi/2$; a more detailed noise analysis is presented in the next section.

Because of the intrinsic susceptibility of the second derivative to high frequency noise, signal filtering is important: the second derivative of x is proportional to $-\omega^2 x(\omega)$ so the high frequency noise in the input is amplified, thus the SNR for \ddot{x} is degraded relative to that for x . To avoid this the signal should be filtered by means of bandpass filter of order not less than 2 near ω_0 with bandwidth $\Delta\omega \ll \omega_0$. In practice the limit $\Delta\omega \leq 0.1 \cdot \omega_0$ works well. The analysis for a sampled signal x_i is very similar.

III. FREQUENCY MEASUREMENT FOR NOISY SIGNALS

To analyze the influence of cantilever noise on frequency measurement we examine Eq. (1) in the continuous domain for comparison to the digital domain

$$-(\omega_0 + \omega_n)^2 = \frac{T * \left[(x + x_n) \frac{d^2}{dt^2} (x + x_n) \right]}{T * [(x + x_n)^2]}, \quad (2)$$

where ω_n is the frequency measurement noise resulting from a displacement noise x_n , which we take to be small compared to x , and $T(t) * f(t)$ signifies the convolution of $f(t)$ with $T(t)$

$$T(t) = \begin{cases} 0, & t < 0 \\ 1/T, & 0 \leq t < T \\ 0, & t \geq T \end{cases}.$$

This is equivalent to a sliding average of $f(t)$ over a time period T and emulates the summation in Eq. (1). The coefficient $1/T$ is used for convenience and does not influence the ratio in Eq. (1). Neglecting terms of order x_n^2 (since $x_n \ll x_0$) we obtain

$$-(\omega_0 + \omega_n)^2 = \frac{T * (x\ddot{x} + x\ddot{x}_n + x_n\ddot{x})}{T * (x^2 + 2xx_n)}.$$

The equation of motion for an oscillating cantilever is

$$\ddot{x}(t) + \frac{\gamma}{m} \dot{x}(t) + \omega_0^2 x(t) = \frac{F_{\text{ex}}}{m},$$

where m is the cantilever mass, γ the damping coefficient, ω_0 its frequency, and F_{ex} the external force applied to the cantilever. In the steady state the cantilever oscillates with constant amplitude, and the external excitation force compensates the attenuation, so, if we exclude pulsed or very noisy external forces we can then assume $T * F_{\text{ex}} = T * \gamma \dot{x}(t)$, and we get

$$-(\omega_0 + \omega_n)^2 = \frac{T * (-\omega_0^2 x^2 + x \ddot{x}_n - \omega_0^2 x x_n)}{T * (x^2 + 2x x_n)}.$$

Fluctuating external forces may increase detection noise. Now

$$\begin{aligned} (\omega_0 + \omega_n)^2 &= \frac{\omega_0^2 T * x^2 \left[1 - \frac{T * (x \ddot{x}_n)}{\omega_0^2 T * x^2} + \frac{T * (x x_n)}{T * x^2} \right]}{T * x^2 \left(1 + 2 \frac{T * (x x_n)}{T * x^2} \right)} \\ &\approx \omega_0^2 \left[1 - \frac{T * (x \ddot{x}_n)}{\omega_0^2 T * x^2} - \frac{T * (x x_n)}{T * x^2} \right], \\ \omega_n &= -\frac{\omega_0}{2T * x^2} T * \left[x \left(\frac{\ddot{x}_n}{\omega_0^2} + x_n \right) \right]. \end{aligned} \quad (3)$$

We take the cantilever signal to be $x(t) = x_0 e^{i\omega_0 t}$ to simplify later Fourier analysis. By definition, the average of $x^2(t)$ is $T * x^2 = x_0^2$. For simplicity we denote the Fourier transforms of x_n and ω_n as $x_n(\omega)$ and $\omega_n(\omega)$, etc. Fourier transformation of Eq. (3) gives

$$\begin{aligned} \omega_n(\omega) &= -\frac{\omega_0}{2x_0} T(\omega) \cdot \left[\delta(\omega - \omega_0) * \left(\frac{\omega_0^2 - \omega^2}{\omega_0^2} x_n(\omega) \right) \right] \\ &= -\frac{\omega_0}{2x_0} T(\omega) \cdot \left[\frac{-\omega^2 + 2\omega\omega_0}{\omega_0^2} x_n(\omega - \omega_0) \right]. \end{aligned}$$

We seek to measure dc value ω_0 and we are interested in noise in this immediate vicinity: $\omega \ll \omega_0$

$$\omega_n(\omega) = -\frac{1}{x_0} T(\omega) \cdot \omega x_n(\omega - \omega_0).$$

We expect the following frequency dependence for x_n :

$$x_n(\omega) = \frac{F_n/m}{\omega_0^2 - \omega^2 + i \frac{\omega\omega_0}{Q}} + I_n,$$

where F_n is the cantilever thermomechanical force noise⁶ and I_n is the effective interferometer noise (taken to be white in the band of interest). We consider white noise in the form $F_n = F_{n0} e^{i\phi_n(\omega)}$ and $I_n = I_{n0} e^{i\psi_n(\omega)}$, where F_{n0} and I_{n0} are real constants and ϕ_n and ψ_n are real random phases. Then

$$\begin{aligned} \omega_n(\omega) &= \frac{1}{2x_0} T(\omega) \cdot \left(\frac{F_n}{m\omega_0} - 2\omega I_n \right) \\ &= \frac{1}{2x_0} T(\omega) \cdot \left(\frac{F_n}{k} \omega_0 - 2\omega I_n \right), \end{aligned}$$

hence the frequency noise for given cantilever and readout noise levels is given by

$$\frac{\omega_n(\omega)}{\omega_0} = \frac{1}{x_0} T(\omega) \cdot \left(\frac{F_n}{2k} - \frac{\omega}{\omega_0} I_n \right). \quad (4)$$

This result is in agreement with results for frequency/phase noise of electronic oscillators.⁷ For frequency noise induced solely by thermomechanical noise (i.e., if I_n is negligible) one can arrive at a result for ω_n more easily. Since ω_0^2

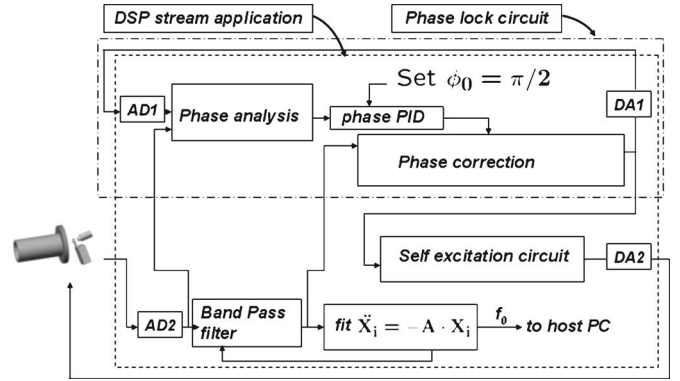


FIG. 1. Schematic diagram of the frequency detection and self oscillation circuits; both are implemented by the digital signal processing (DSP) board. The large box defined by the dashed line contains the functional units implemented as a DSP stream application, and the small box indicated with a dash-dot line contains the elements of the digital phase-lock circuit.

$= k/m$ and $\omega_n/\omega_0 = k_n/2k$, where k_n is the effective spring constant noise ($k_n = F_n/x_0$) we get $\omega_n/\omega_0 = F_n/(2kx_0)$ in agreement with the result in Eq. (4).

IV. IMPLEMENTATION OF FREQUENCY DETECTION SCHEME

We have implemented this frequency detection scheme in a magnetic resonance force microscopy (MRFM) instrument using a digital signal processor (DSP) board.⁸ Figure 1 shows a schematic diagram of the frequency detection setup.

A 1024 point digital record of the digitized cantilever displacement (from an optical fiber interferometer) signal is collected and digitally filtered with a fourth-order IIR Butterworth bandpass filter (this signal is designated “ x ” in Fig. 1). The second time derivative \ddot{x} is calculated and \ddot{x} versus x is fit to a line; the slope of the line gives the cantilever frequency; frequency values are obtained continuously once every ~ 4 ms (1024 points obtained at a 250 kHz sampling rate), and this result is recorded in the host computer.

To relate frequency shift to the force the cantilever must execute constant amplitude oscillations at its resonance frequency. This is achieved by a digital positive feedback circuit in which the cantilever serves as the frequency determining element; Fig. 1 shows the implementation of this circuit. A replica of the filtered input signal is passed to the output with a $\pi/2$ phase shift (corrected by a proportional control circuit with a 100 ms characteristic time constant) imposed to create an output phase locked to the cantilever signal. This signal can have an arbitrary (time varying, if desired) amplitude. This signal can be used to generate other needed signals that must be referenced to the cantilever.

V. EXPERIMENTAL RESULTS

We have detected MRFM signals with high sensitivity and user defined bandwidth using this method. The frequency noise of the cantilever measured using the DSP frequency detector is shown in Fig. 2. This noise includes contributions from the cantilever thermomechanical noise x_{th} and the effective interferometer noise x_{int} [see Fig. 2(a)]. Relative to the thermomechanical noise x_{th} , x_{int} decreases

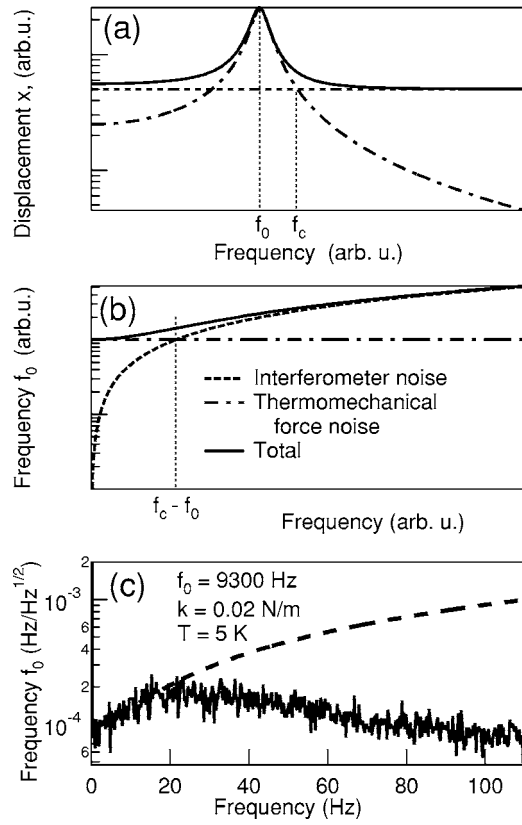


FIG. 2. (a) Typical cantilever displacement noise. (b) Cantilever displacement noise after conversion to frequency noise using the frequency evaluation procedure described in the text. The optimal mechanical detector bandwidth $f_c - f_0$ is indicated (see text). (c) Measured frequency noise for the Veeco cantilever used in the ESR/MRFM experiment (shown in Fig. 3); this measurement was made at $T = 5$ K with $x_0 \approx 100$ nm. The dashed line shows the theoretical noise given by Eq. (4); we used the values $F_n = 4 \times 10^{-17}$ N/ $\sqrt{\text{Hz}}$ and $I_n = 8 \times 10^{-13}$ m/ $\sqrt{\text{Hz}}$. The experimental noise is attenuated at higher frequency by a bandpass filter applied to the cantilever signal. For all graphs the vertical and horizontal scales are logarithmic and linear, respectively.

with decreasing frequency offset from the cantilever resonance frequency f_0 because x_{th} is resonantly enhanced within $\Delta f = f_0/Q$ of f_0 whereas x_{int} is essentially constant; f_c denotes the frequency above which the interferometer noise exceeds thermomechanical noise and defines the optimal bandwidth of the mechanical detector.

After applying our frequency detection procedure these noise sources are converted to frequency noise as shown in Fig. 2(b) [see Eq. (4)]. Figure 2(c) shows the experimentally measured frequency noise. The cantilever⁹ (spring constant $k = 0.02$ N/m, resonance frequency $f_0 \approx 9300$ Hz, and quality factor $Q \approx 55\,500$) is driven to maintain constant oscillation amplitude $x_0 \approx 100$ nm and measurements were made at $T = 5$ K in vacuum. The measured frequency noise $f_n = 1 \times 10^{-4}$ Hz/ $\sqrt{\text{Hz}}$ expressed in terms of an effective force noise is

$$F_n = \frac{2f_n}{f_0} kx_0 = 4 \times 10^{-17} \frac{\text{N}}{\sqrt{\text{Hz}}}$$

and is the same as our estimate for the thermomechanical noise⁶ for this cantilever:

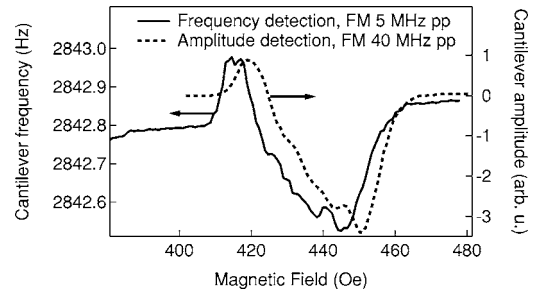


FIG. 3. MRFM/ESR signal obtained from a film sample of DPPH. The signal was obtained by detecting the shift in the cantilever eigenfrequency that occurs as a consequence of the oscillatory force exerted on the cantilever in the electron spin resonance experiment (solid curve; refer to the left-hand axis). This is compared to the same signal detected by the conventional approach of detecting the cantilever oscillation amplitude after excitation by the spin resonance force (dashed curve, right-hand axis). The frequency signal has larger bandwidth than the amplitude signal whose bandwidth is limited by the cantilever time constant.

$$F_{\text{th}} = \sqrt{4\gamma k_b T} = \sqrt{\frac{2k k_b T}{\pi Q f_0}} \approx 4 \times 10^{-17} \text{ N}/\sqrt{\text{Hz}}.$$

Hence the effective noise is dominated by F_{th} and the noise contributed by the detection circuit is negligible.

A MRFM electron spin resonance (MRFM/ESR) signal from a sample of DPPH (Ref. 10) attached to a SiN cantilever⁹ is shown in Fig. 3. The signal force is due to the $\sim 10^2$ T/m magnetic field gradient of a stationary probe magnet brought close to the sample. The sample magnetization was cyclically saturated by modulating the frequency of the microwave field at f_0 . The solid curve in Fig. 3 shows the DPPH electron spin resonance signal obtained by frequency detection. The FM modulation depth was 5 MHz peak to peak and the microwave power was ~ 20 dBm. For comparison we show the MRFM/ESR signal obtained by traditional amplitude detection (dashed curve) at the same microwave power but with larger FM modulation depth. Both signals have similar features demonstrating the high fidelity of our frequency detection method.

VI. CONCLUSION

We demonstrate a previously untried method for digital frequency evaluation of periodic signals and present a noise analysis for this method when applied to a microcantilever force sensor signal. We have demonstrated real-time frequency evaluation of cantilever signals with high precision. Since the added noise is negligible compared to thermal force noise of the cantilever, the force resolution is close to thermal limit of cantilever itself. Beyond this, the DSP approach is easily extended to encompass an integrated MRFM measurement system that includes a self-excitation circuit, a frequency detector, and signals that control modulation of the rf signals that can be phase locked to the cantilever signal. This integrated system was demonstrated in a measurement of the MRFM/ESR signal from a DPPH sample and its performance evaluated.

This work was supported by the US Department of Energy through grant DE-FG02-03ER46054.

- ¹J. A. Sidles, J. L. Gaarbini, K. J. Bruland, D. Rugar, O. Zuger, S. Hoen, and C. S. Yannoni, *Rev. Mod. Phys.* **67**, 249 (1995).
- ²D. Rugar, R. Budakian, H. J. Mamin, and B. W. Chui, *Nature* **430**, 329 (2004).
- ³K. J. Bruland, J. L. Garbini, W. M. Dougherty, and J. A. Sidles, *J. Appl. Phys.* **80**, 1959 (1996).
- ⁴T. R. Albrecht, P. Grütter, D. Horne, and D. Rugar, *J. Appl. Phys.* **69**, 668 (1991).
- ⁵T. R. Albrecht, P. Grütter, D. Rugar, and D. P. E. Smith, *Ultramicroscopy* **42–44**, 1638 (1992).
- ⁶M. V. Salapaka, H. S. Bergh, J. Lai, A. Majumdar, and E. McFarland, *J. Appl. Phys.* **81**, 2480 (1997).
- ⁷W. P. Robins, *Phase Noise in Signal Sources: Theory and Applications* (Peter Peregrinus Ltd., London, 1982), p. 45, Eq. 4.6.
- ⁸Innovative Integration “Toro” board, based on the Texas Instrument floating point DSP TMS320C67x, 16 analog I/O channels, 16 bit dynamic range, 250 kHz analog signal sampling rate.
- ⁹MPP-32100-50 Light Contact Mode Silicon Probe, Veeco Metrology LLC.
- ¹⁰Diphenyl picryl hydrazyl from Sigma-Aldrich, Product Number: 257621.